Template Removal via Boudouard Equilibrium Allows for Synthesis of Mesostructured Molybdenum Compounds

Martin Schieder,[a] Carina Bojer,[a] Julia vom Stein,[b] Sebastian Koch,[a] Thomas Martin,[a] Holger Schmalz[c], Josef Breu*[a], Thomas Lunkenbein*[d]

Abstract: Oxidative thermal removal of the polymeric templates is not trivial for molybdenum oxides and hampers mesostructuring of this material. At ambient oxygen fugacity Mo(VI) is the thermodynamically stable oxidation state and sublimation of MoO_3 leads to a quick loss of the mesostructure due to Oswald ripening. Taking advantage of the Boudouard equilibrium allows to fix the oxygen fugacity at a level where non-volatile MoO_{2-x} is stable while carbonaceous material may be oxidized by CO_2. Mesostructured MoO_{2-x} can be chemically converted to MoO_3 or MoN under retention of the mesostructure.

Molybdenum oxides, carbides or nitrides are applied in several fields ranging from heterogeneous catalysis[1-3] over electrocatalysts for hydrogen evolution reaction[4] and electrochromic displays[5] to charge storing anodes in batteries.[6]
However, the catalytic activity of these compounds is limited by the low surface area and/or porosity. To increase specific surface area, nanocrystalline metal oxide precursors may be aligned at the mesoscale.[7-11] This can be achieved by a template assisted route in the presence of surfactants or block copolymers.[12-14] To fully exploit the potential of these materials for most applications the template has to be removed. Traditionally, the removal of the carbonaceous material can be achieved by a subsequent calcination step at elevated temperatures in oxygen containing atmosphere. Other reports involve an additional heat treatment step, in which the organic template is first converted into a rigid carbon scaffold followed by a second calcination in air. This method is often referred to as combined assembly of soft and hard (CASH) method and ensures a stabilization of the oxidic walls during crystallization and sufficiently supports the retention of the mesostructure.[15] As we could show, the CASH method for instance gives access to 1-dimensional (1D) WO_3 nanotubes,[11] and to 1D as well as hexagonal ordered molybdenum carbide/ carbon nanocomposites (MoC/C).[16] For microtomed hexagonally ordered molybdophosphoric acid (H_3PMo)/polymer films, the template may be removed by plasma treatment on a transmission electron microscopy (TEM) grid to obtain mesoporous H_3PMo.[17] This method is, however, limited to thin films (< ~50 nm) and some residual carbon is needed to glue the H_3PMo moieties. Attempts to synthesize carbon-free bulk samples of mesoporous molybdenum oxides using one of the above mentioned carbon removal techniques failed. At high temperatures ambient oxygen fugacity will yield MoO_3 which readily undergoes vapor-phase sintering that is accompanied by fast Ostwald ripening into micrometer sized particles resulting in a collapse of the mesostructure (Figure S1).
Controlling oxygen fugacity during template removal is certainly a yet neglected parameter to overcome this problem. At lower oxygen partial pressure ($p(O_2)$) MoO_{2-x} is thermodynamically favored over MoO_3 (Figure 1b).[18] The former crystallizes in a distorted rutile structure and is electrically conductive.[19] In addition, MoO_{2-x} exhibits no appreciable vapor pressure[20] (Figure 1a) and the collapse of the mesophase may therefore be avoided, while the $p(O_2)$ is still high enough to ensure removal of the carbon scaffold (Figure 1b).
Herein we describe a synthetic protocol towards 1D mesoporous MoO_{2-x} nanowires by endotemplating followed by subsequent carbothermal treatment in inert atmosphere and calcination under controlled $p(O_2)$. MoO_{2-x} was subsequently converted into MoN and MoO_3 while preserving the mesostructure. Ammonium dimolybdate ($(NH_4)_2Mo_2O_7$, ADM) was used as molybdenum precursor. 1D polyelectrolytic core-crosslinked poly(butadiene-*block*-2-vinylpyridine) (PB-*b*-P2VP) was employed as soft template and simultaneously as carbon source in the carburization reaction. We will demonstrate that the key to the successful synthesis of mesostructured MoO_{2-x} was oxidation of MoC/C nanocomposites in CO_2 atmosphere. This way $p(O_2)$ is fixed via the Boudouard equilibrium (I) whereby carbonaceous material is removed while keeping Mo at its +IV oxidation state:

$$C + CO_2 \rightleftarrows 2\,CO \qquad (I)$$

Scheme 1 summarizes the approach.

PB-*b*-P2VP (60 $kgmol^{-1}$; 81 wt.-% P2VP, PDI 1.02) self-assembles after solvent evaporation into hexagonally ordered PB cylinders in a P2VP matrix. After crosslinking the PB moieties the film can be dispersed in HCl (0.001 M) into rigid cylindrical nanobrushes.[9,15] Details on the synthesis and characterization are given in the supporting information and recent reports, respectively.[11,21,22]

[a] M. Schieder,[+] C. Bojer,[+] S. Koch, T, Martin, Prof. Dr. J. Breu
Lehrstuhl für Anorganische Chemie I
Universität Bayreuth
Universitätsstraße 30, 95440 Bayreuth
E-mail: josef.breu@uni-bayreuth.de
[b] J. vom Stein
Abteilung für Heterogene Katalyse
Max-Planck Institut für Kohlenforschung
Kaiser-Wilhelm-Platz 1, 45470 Mühlheim a.d. Ruhr
[c] Dr. H. Schmalz
Lehrstuhl für Makromolekulare Chemie II
Universität Bayreuth
Universitätsstraße 30, 95440 Bayreuth
[d] Dr. T. Lunkenbein
Abteilung für Anorganische Chemie
Fritz-Haber Institut der Max-Planck Gesellschaft
Faradayweg 4-6, 14195 Berlin
E-mail: lunkenbein@fhi-berlin.mpg.de
[+] M.S. and C.B. contributed equally to this work.

Supporting information for this article is given via a link at the end of the document.

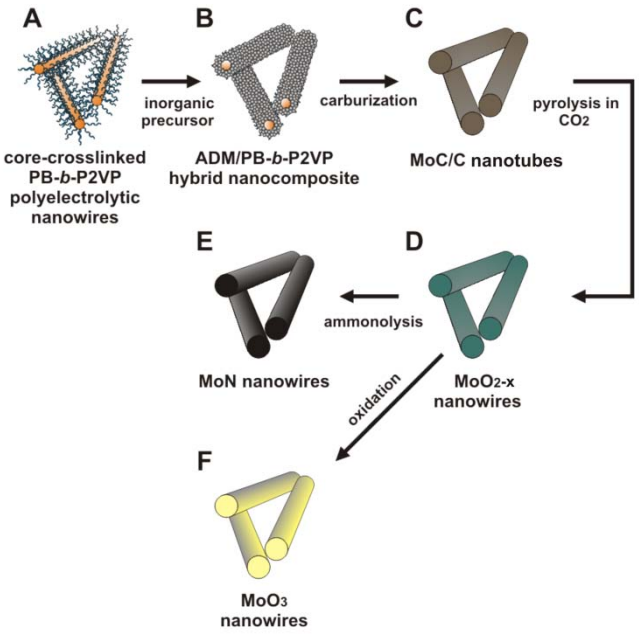

Scheme 1. Synthesis of PB-*b*-P2VP nanowires by self-assembly of PB-*b*-P2VP block copolymer, crosslinking and dissolution of the nanowires (A), addition of $(NH_4)_2Mo_2O_7$ (ADM) precursor for ADM/PB-*b*-P2VP nanocomposite formation (B), carburization to MoC/C (C), pyrolysis in CO_2 atmosphere to MoO_{2-x} (D) nitridation to MoN (E) or oxidation to MoO_3 nanowires(F).

Structural assignment of the as-synthesized ADM/PB-*b*-P2VP nanocomposites was accomplished by TEM measurements (Figure 2). The SEM and TEM micrograph reveals 1D cylindrical nanocomposites with diameters of (41 ± 7) nm. The diffuse ring pattern of the selected area electron diffraction measurement (SAED) (Figure 2, inset) of the ADM/PB-*b*-P2VP nanocomposites and the powder X-ray diffraction (PXRD) data (Figure S2A) indicate an amorphous material. The N_2 physisorption isotherms (Figure S5A) of the as-synthesized material are characteristic for interparticular pores in non-woven mesostructures from which a specific BET surface area of 69 m^2g^{-1} can be derived. This is in the expected range for 1D polyoxomolybdate based nanocomposites.[21,22]

At ambient oxygen fugacity Mo(VI) is the thermodynamically stable oxidation state (Figure 1b). Unfortunately, the equilibrium partial pressure of MoO_3 is significant and at any temperature orders of magnitude higher than of MoO_{2-x} (Figure 1a). Consequently, MoO_3 readily sublimes at temperatures usually applied during oxidative template removal by forming polymeric $(MoO_3)_x$ species[23-25] according to:

$$x\ MoO_3(s) \rightarrow (MoO_3)_x(g) \quad (x= 3, 4, 5) \qquad (II)$$

Rapid gas phase sintering yields quickly micrometer sized crystals. The speed of vaporization can be increased by the presence of steam in the carrier gas (Figure 1a) via formation of gaseous molybdenum oxyhydroxide $(MoO_2(OH)_2)$.[24]

$$MoO_3(s) + H_2O(g) \rightarrow MoO_2(OH)_2(g) \qquad (III)$$

Contrary to MoO_3, MoO_{2-x} does not possess any appreciable vapor pressure in the medium temperature regime (Figure 1a).[20,23] Consequently, the described dilemma can be avoided by oxidizing the carbon scaffold at oxygen fugacities where MoO_2 is the stable phase.

As shown in the Ellingham diagram (Figure 1b) the desired oxygen fugacity can be thermodynamically achieved by using CO_2 as oxidation agent. In the temperature regime up to 1051 K carbon can be oxidized by CO_2 via the Boudouard equilibrium, whereas MoO_{2-x} can neither be oxidized to MoO_3 nor be reduced to Mo by the generated CO. By fixing $p(O_2)$ this way, we could remove carbon and simultaneously preserve the mesostructure of MoO_2.

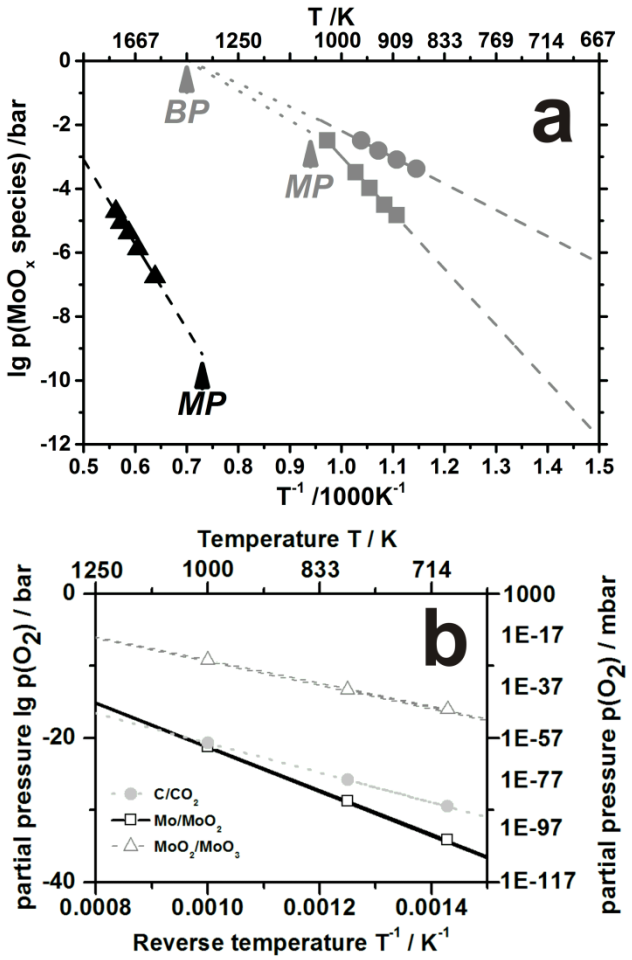

Figure 1. a: Partial pressure of volatile MoO_x species as function of temperature, grey: $(MoO_3)_{3(g)}$ (bottom curve) and $MoO_2(OH)_{2(g)}$ (top curve) over MoO_3.[20,23-25] Relevant MoO_x species vary with humidity of the carrier gas. The top grey curve was measured in 100% steam, whereas the bottom one was obtained in dry atmosphere. Other oligomeric gas phase $(MoO_3)_x$ species are omitted. Black: partial pressure of different MoO_x species over MoO_2. MP and BP denote the melting point and boiling point.[20,24] b: Calculated Ellingham diagram for C/CO_2, Mo/MoO_2 and MoO_2/MoO_3 equilibrium lines.

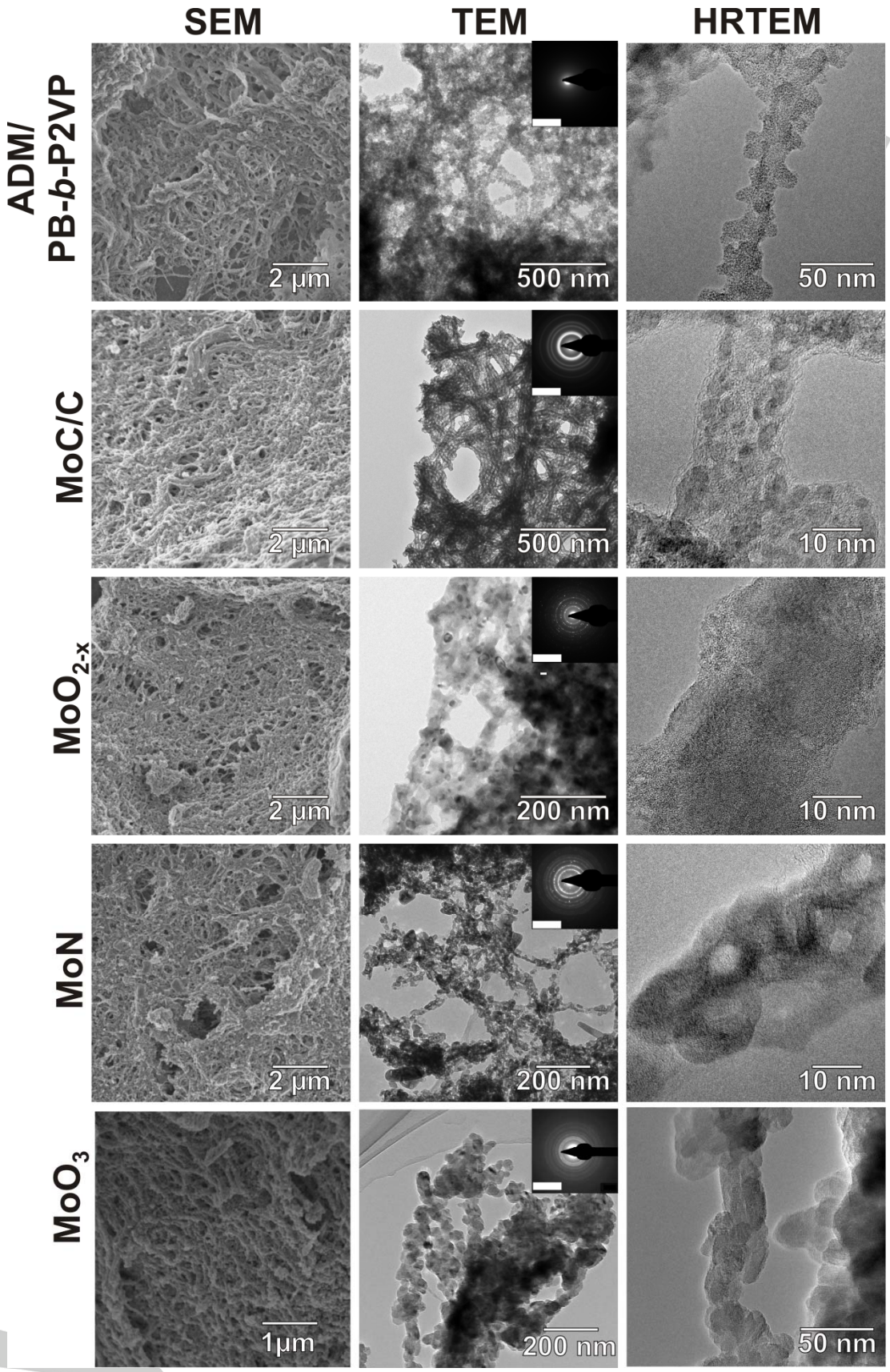

Figure 2. SEM, TEM, HRTEM images and SAED (insets scalebar is 10 nm^{-1}) of ADM/PB-*b*-P2VP nanocomposite, MoC/C after carburization, MoO_{2-x} after pyrolysis in CO_2 atmosphere, MoN after ammonolysis and MoO_3 after oxidation of MoO_{2-x} in oxygen.

Removal of the polymeric template was accomplished by two calcination steps:

First, the sp^2-hybridized carbon atoms of the ADM/PB-*b*-P2VP nanocomposites were converted in argon atmosphere at 973 K into a carbonaceous scaffold which stabilizes and lines the inorganic walls (Scheme 1C). Further details on this carburization reaction can be found in previous reports.[10,21] The carburization resulted in 1D MoC/C nanocomposites with diameters of 33 ± 5 nm as derived from TEM images (Figure 2) and MoC or oxycarbide nanoparticles in the walls, which are embedded in carbon. In addition, TEM reveals a caterpillar like structure of the individual MoC/C cylinders. The observations made by TEM are in line with previous reports on molybdenum oxycarbide/carbon nanocomposites.[11,22] Phase analysis by PXRD (Figure S2B) revealed broad reflections, which can be attributed to a nanocrystalline face-centered cubic cell of MoC_{1-x} or to a molybdenum oxycarbide phase.[16,22] The SAED pattern of the MoC/C nanocomposite further corroborated the formation of nanocrystalline carbide species (insets Figure 2, Figure S4). N_2 physisorption experiments of the MoC/C nanocomposites (Figure S5a) revealed a similar isotherm and the same type of hysteresis as for ADM/PB-*b*-P2VP nanocomposites supporting the retention of the non-woven network with inter-particular pores in a non-woven array of 1D mesostructures with BET surface area of 240 m^2g^{-1}. This high surface area may be attributed to the formation of a microporous carbon framework.

Second, the MoC/C nanocomposite was subjected to a thermal treatment in CO_2 atmosphere (Scheme 1D). Thermogravimetric measurement coupled with mass spectroscopy (TG-MS) of MoC/C in CO_2 atmosphere (Figure 3) confirmed thermodynamical considerations. Thermodynamically, it is expected that at temperatures < 1051 K CO_2 will concomitantly be capable to oxidize residual carbon leading to a weight loss and to oxidize MoC to MoO_{2-x} which is related with a weight gain. The TG will therefore reflect a superposition of two reactions. In line with these expectations, CO evolution commences at around 750 K and peaks at 1033 K.

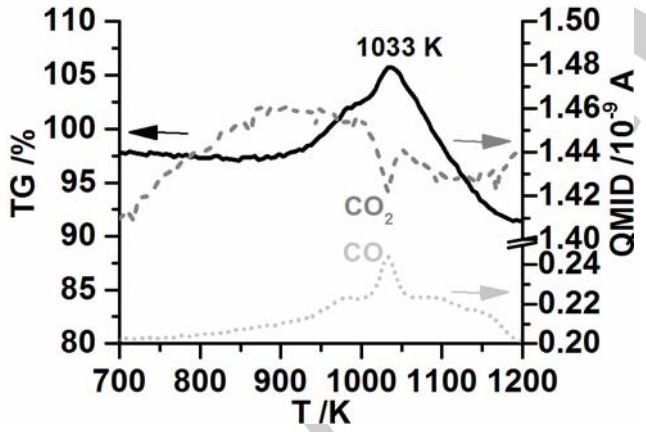

Figure 3. TG-MS measurement of MoC/C (black) and quasi multiple ion detection (QMID) signals of CO_2 (m/z = 44, dark grey) and CO (m/z = 28, light grey) in CO_2 atmosphere.

Despite this superposition, at around 950 K an onset of a weight gain is observed with a maximum at around 1033 K indicating that the conversion of MoC to MoO_{2-x} dominates at this temperature. Above 1033 K a steep mass loss is observed. This may be attributed to a superposition of oxidation of carbonaceous material and reduction of MoO_{2-x} to suboxides for which no reliable thermodynamic data are available and which therefore have been omitted in Figure 1. Above 1051 K the C/CO_2 line crosses the Mo/MoO_2 line (Figure 1b) suggesting that then even the reduction of MoO_{2-x} to metallic Mo will be favored thermodynamically. To further narrow down the maximum temperature for the calcination step, temperature controlled PXRD experiments were performed in CO_2 atmosphere (Figure S3). Up to 873 K all reflections observed can be assigned to either MoO_{2-x} or MoC. At 973 K only MoO_{2-x} is observed and above this temperature additional reflections attributed to suboxides start appearing. Based on PXRD and TG analysis, MoC/C nanocomposites were therefore pyrolized at 973 K in CO_2 atmosphere.

SEM and TEM micrographs (Figure 2) revealed the preservation of the 1D wire-like mesostructure with a slightly decreased diameter of 32 ± 6 nm. The PXRD patterns (Figure S2c) confirm that monoclinic MoO_{2-x} was formed. The broadening of the reflections indicates the presence of nanocrystalline material. However, the spotted ring pattern in the SAED pattern (Figure 2, inset) indicates a slight increase of the size of the coherent scattering domains of MoO_{2-x}. While confirming the formation of monoclinic MoO_{2-x} (Figure S4).

N_2 physisorption measurements (Figure S5C) of the MoO_{2-x} nanowires revealed a mesoporous type II isotherm with H4 hysteresis indicating interparticle mesopores in the nanowires. The BET surface area decreased from 240 m^2g^{-1} (MoC/C) to 152 m^2g^{-1} for the MoO_{2-x} nanowires. The decrease in surface area can be explained by the removal of the microporous carbon framework as CO, the volume change related to the conversion of MoC to MoO_{2-x}, as well as a certain degree of sintering occurring during the second heat treatment. The remaining carbon content was estimated by elemental analysis to be 1.2 wt.-%, which is a reduction of 96% compared to the ADM/PB-*b*-P2VP (Table S1). Raman measurements of the MoO_{2-x} nanowires also confirmed a significant release of carbon through the Boudouard equilibrium (Figure S7).

The robustness of MoO_{2-x} nanowires obtained is evidenced by chemical conversions under retention of the mesostructure. MoO_{2-x} can easily be oxidized with oxygen to MoO_3 with preservation of the mesostructure and a surface area of 50 m^2g^{-1} at a temperature (573 K) low enough to prevent gas phase sintering (Figure 2, Figure S2E).

MoO_{2-x} was furthermore transformed into MoN nanowires via ammonolysis (Figure S2d). As a result of the higher density of the nitride (9.2 cm^3g^{-1}) the BET surface area dropped to 36 m^2g^{-1} irrespective of the preservation of the mesostructure (Figure 2 and Figure S5D). The catalytic activity of the MoN nanowires was tested in the decomposition of NH_3. Preliminary activity tests revealed an activation energy of 131 kJ mol^{-1} (Figure S6), which is in-between our previous results obtained for 1D MoC/C (127 kJ mol^{-1}) and hexagonally ordered MoC/C (156 kJ mol^{-1}) nanocomposites, respectively.[16,22]

In summary, we have realized a reaction pathway for mesostructured MoO_{2-x}, MoN and MoO_3 nanowires. The synthesis concept involves two heating steps and carbon removal is assisted by the Boudourad equilibrium. It is the Boudouard equilibrium, which enables avoidance of vapor phase sintering of MoO_3 into micrometer sized crystals which is accompanied by the loss of the mesostructure. The use of CO_2 as mild oxidation agent fixes $p(O_2)$ at a level where Mo(IV) is thermodynamically stable while carbonaceous material is oxidized to CO. In addition, at the applied temperature regime the reduction potential of the generated CO is low enough to

avoid further reduction of MoO_{2-x} to sub-stoichiometric oxides or elemental Mo. The resulting MoO_{2-x} nanowires show high specific surface area and the robust mesostructure allows for chemical conversion into MoO_3 and MoN. MoN nanowires are active in the catalytic decomposition of NH_3. We can, therefore, label our approach as a general pathway towards mesostructured refractory materials.

Acknowledgements

The authors wish to thank Professor R. Schlögl (Fritz-Haber Institute, Berlin) for access to HRTEM, Prof. F. Schüth (Max Planck Institute, Mülheim) for catalytic tests. This work was supported by the German Science Foundation (Grant SFB 840).

Keywords: Boudouard equilibrium • nanowires • molybdenum oxide • mesostructuring • oxygen fugacity

Supporting Information:
PXRD measurements, N_2 physisorption measurements and a table with structural details of as-synthesized ADM/PB-*b*-P2VP, MoC/C, MoO_{2-x}, MoO_3 and MoN nanowires; NH_3 decomposition test of MoN with Arrhenius plot; Raman measurement of MoC/C and MoO_2 nanowires.

[1] X. Chen, T. Zhang, M. Zheng, Z. Wu, W. Wu, C. Li, *J. Catal.* **2004**, *224*, 473–478.
[2] T. Ressler, A. Walter, Z.-D. Huang, W. Bensch, *J. Catal.* **2008**, *254*, 170-179.
[3] Z. Huang, W. Bensch, W. Sigle, P. A. van Aken, L. Kienle, T. Vitoya, H. Modrow, T. Ressler, *J Mater Sci* **2008** *43*, 244-253.
[4] H. Bin Wu, B. Y. Xia, L. Yu, X.-Y. Yu, X. W. (David) Lou, *Nat. Commun.* **2015**, *6*, 6512.
[5] N. A. Chernova, M. Roppolo, A. C. Dillon, M. S. Whittingham, *J. Mater. Chem.* **2009**, *19*, 2526.
[6] T. Brezesinski, J. Wang, S. H. Tolbert, B. Dunn, *Nat. Mater.* **2010**, *9*, 146–151.
[7] R. S. Yelamanchili, Y. Lu, T. Lunkenbein, N. Miyajima, L. T. Yan, M. Ballauff, J. Breu, *Small* **2009**, *5*, 1326–1333.
[8] M. Müllner, T. Lunkenbein, N. Miyajima, J. Breu, A. H. E. Müller, *Small* **2012**, *8*, 2636–2640.
[9] M. Müllner, T. Lunkenbein, J. Breu, F. Caruso, A. H. E. Müller, *Chem. Mater.* **2012**, *24*, 1802–1810.
[10] M. Müllner, T. Lunkenbein, M. Schieder, A. H. Gröschel, N. Miyajima, M. Förtsch, J. Breu, F. Caruso, A. H. E. Müller, *Macromolecules* **2012**, *45*, 6981–6988.
[11] M. Schieder, T. Lunkenbein, T. Martin, W. Milius, G. Auffermann, J. Breu, *J. Mater. Chem. A* **2013**, *1*, 381–387.
[12] D. R. Rolison, *Science* **2003**, *299*, 1698–1701.
[13] S. Polarz, M. Antonietti, *Chem. Commun.* **2002**, *0*, 2593–2604
[14] G. Kickelbick, *Prog. Polym. Sci.* **2003**, *28*, 83–114
[15] J. Lee, M. Christopher Orilall, S. C. Warren, M. Kamperman, F. J. DiSalvo, U. Wiesner, *Nat. Mater.* **2008**, *7*, 222–228.
[16] T. Lunkenbein, D. Rosenthal, T. Otremba, F. Girgsdies, Z. Li, H. Sai, C. Bojer, G. Auffermann, U. Wiesner, J. Breu, *Angew. Chemie Int. Ed.* **2012**, *51*, 12892–12896.
[17] T. Lunkenbein, M. Kamperman, M. Schieder, S. With, Z. Li, H. Sai, S. Förster, U. Wiesner, J. Breu, *J. Mater. Chem. A* **2013**, *1*, 6238.
[18] H. J. Hwang, M. Toriyama, T. Sekino, K. Niihara, *J. Eur. Ceram. Soc.* **1998**, *18*, 2193–2199.
[19] A. Magnéli, G. Andersson, *Acta Chem. Scand.* **1955**, 1378–1381.
[20] R. P. Burns, G. DeMaria, J. Drowart, R. T. Grimley, *J. Chem. Phys.* **1960**, *32*, 1363.
[21] T. Lunkenbein, M. Schieder, C. Bojer, A. H. E. Müller, J. Breu, *Z. Phys. Chem.* **2012**, *226*, 815–826.
[22] M. Schieder, T. Lunkenbein, C. Bojer, M. Dulle, J. vom Stein, G. Auffermann, T. Löbling, J. Schöbel, H. Schmalz, J. Breu, *Z. Anorg. Allg. Chem.* **2015**, *641*, 1829–1834.
[23] P. E. Blackburn, M. Hoch, H. L. Johnston, *J. Phys. Chem.* **1958**, *62*, 769–773.
[24] O. Glemser, R. V. Haeseler, *Z. Anorg. Allg. Chem.* **1962**, *316*, 168–181.
[25] J. Berkowitz, M. G. Inghram, W. a. Chupka, *J. Chem. Phys.* **1957**, *26*, 842.

Entry for the Table of Contents (Please choose one layout)

Layout 1:

COMMUNICATION

Mesostructuring of molybdenum compounds is hampered by fast gas phase sintering of MoO_3 obtained during the oxidative removal of templates. Taking advantage of the Boudouard equilibrium allows for maintaining the oxygen fugacity at a level where non-volatile MoO_{2-x} is stable while carbonaceous material is oxidized by CO_2. Mesostructured MoO_{2-x} can subsequently be converted to MoO_3 or MoN under retention of the mesostructure.

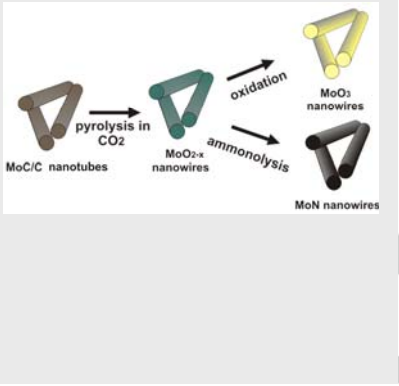

*Author(s), Corresponding Author(s)**

Page No. – Page No.

Title